Supporting Information

pH matters when reducing CO_2 in an electrochemical flow cell

Zishuai Zhang,[1] Luke Melo,[1] Ryan Jansonius,[1] Faezeh Habibzadeh,[1] Edward R. Grant,[1] Curtis P. Berlinguette[1,2,3,4]*

[1]Department of Chemistry, The University of British Columbia, 2036 Main Mall, Vancouver, British Columbia, V6T 1Z1, Canada.

[2]Stewart Blusson Quantum Matter Institute, The University of British Columbia, 2355 East Mall, Vancouver, British Columbia, V6T 1Z4, Canada.

[3]Department of Chemical and Biological Engineering, The University of British Columbia, 2360 East Mall, Vancouver, British Columbia, V6Y 1Z3, Canada.

[4]Canadian Institute for Advanced Research (CIFAR), 661 University Avenue, Toronto, M5G 1M1, Ontario, Canada

*Corresponding author: Curtis P. Berlinguette (cberling@chem.ubc.ca)

Experimental

Materials

$KHCO_3$ (99%) and K_2CO_3 (99%) were purchased from Alfa Aesar (USA). Silver foam was purchased from Jiangsu Green Materials Hi-Tech. Co. Ltd. (China). Nickel foam (>99.99%) was purchased from MTI Corporation (USA). Ethylenediaminetetraacetic acid (EDTA, 99%) was purchased from Sigma-Aldrich (USA). Fumasep FBM bipolar membranes were purchased from Fuel Cell Store and stored in a 1 M NaCl solution prior to use. Nitric acid (70% W) was purchased from Fisher Scientific (USA). N_2 (99%), CO_2 (99%) and Ar (99.999%) gasses were obtained from Praxair Canada Inc.. The Sapphire windows were purchased from Thorlabs (WG30503, i.d. 12.7 mm). A CH instrument 660D potentiostat (USA) equipped with an amp booster was used for all electrolysis experiments. The gas chromatograph (GC, Perkin Elmer, Clarus 580) was equipped with a packed MolSieve 5 Å column and a packed HayeSepD column. CO and H_2 were detected by a flame ionization detector (FID) and a thermal conductivity detector (TCD), respectively. Argon was used as carrier gas and the GC was calibrated for CO and H_2 using a previously reported procedure. [1] Confocal Raman spectra are collected using a fiber coupled Olympus BX-51 microscope with a 785 nm excitation source (Innovative Photonics Solutions IO785MM0350M64F).

Electrode Preparation

The Ag foam (0.085 g cm^{-2}) was treated with dilute nitric acid solution ($v_{nitric\ acid}/v_{water}$=1:3) for 10 s to remove the oxide layer and to increase the electrochemical surface area. The treated Ag foam (0.070 g cm^{-2}) was further washed with deionized (DI) water thoroughly. 3M $KHCO_3$ was used for the final wash to ensure the removal of nitric acid.

Electrochemical Measurement and Product Analysis

A CH Instruments 660D with a picoamp booster was used for all experiments. Electrochemical measurements with a two-electrode system with nickel foam as the anode and Ag foam as the cathode were used. The BPM was used as the membrane to separate anodic and cathodic compartments. The anode electrolyte was 1000 mL of 1.0 M KOH solution delivered by a peristaltic pump at 50 mL min^{-1}. The cathode electrolyte was 125 mL of 3.0 M $KHCO_3$ with 0.02 M ethylenediaminetetraacetic acid (EDTA, 99%, Sigma Aldrich). The headspace of the catholyte solution was purged with N_2 (Praxair, 99.9%) gas at 160 sccm in a sealed flask with an outlet into the flow cell. The catholyte solution was delivered by another peristaltic pump at 25 mL min^{-1} into the flow-cell electrolyzer, which was then vented back into the flask. Fresh electrolyte was used for each set of experiments. The produced gases in the headspace of the cathode electrolyte reservoir were delivered into the GC through tubings and the sampling was done automatically. For the operando Raman measurement setup, a mobile power supply (Keithley 2260-30-72) was used. To investigate the feedstock temperature effect on electrolyzer performance, a water bath was used to heat the feedstock to 40, 60 and 80 °C respectively (measured by a glass thermometer), and the temperatures of bicarbonate solutions at inlet were measured with a 100 Ω platinum resistance temperature dectector (Vishay Beyschlag, PTS060301B100RP100).

Cell Design

The custom-made electrolyzer cell depicted in Figure 1 was built in-house and consisted of housing, gaskets, anode and cathode flow-field plates, supporting layer, a sapphire window and a membrane electrode assembly (MEA). Both the anode housing (6 cm × 6 cm × 0.6 cm) and cathode

housing (6 cm × 6 cm × 0.3 cm) are made from stainless steel and serve to deliver liquid and gas feeds to the anode and cathode, respectively. Stainless steel was chosen for its chemical inertness to both anode and cathode feeds. The acid-stable cathode flow plate and base-stable stainless steel anode flow plate sandwiched the 4 cm^2 MEA. The anode (316 stainless steel, 6 × 6 × 0.6 cm; active area = 4 cm^2) and cathode (grade 2 titanium) flow-field plates (6 × 6 × 0.3 cm; active area = 4 cm^2) contained serpentine channels 1.5 mm wide and 1.5 mm deep with 1-mm ribs. The anode flow-field plate design is similar to a previously reported design for a water electrolyzer.[1] The cathode flow-field plate design is shown in Figure S2. Stainless steel and titanium were chosen for anode and cathode flow plates for their inherent chemical stabilities in basic and acidic conditions, and inactivity towards the OER and CO_2RR. All gaskets are cut from 1.5 mm thick chemical resistant compressible polytetrafluoroethylene (PTFE). The PTFE gaskets have good chemical inertness to cathode and anode feeds and high compressibility, ensuring both liquid and gas-tight seals. The gaskets between the housing and the flow-field plate, on both the anode and cathode sides (PTFE gasket A), have 0.2 mm diameter holes for liquid or gas delivery. The gaskets between the flow-field plate and the MEA have a 2 cm × 2 cm square cut out (PTFE gasket B). The MEA consists of a nickel foam anode (2.5 cm × 2.5 cm), a BPM (3 cm × 3 cm), and a silver foam (2.0 cm × 2.0 cm). The nickel foam served as both the porous layer and OER catalyst in basic conditions, and the silver foam were used to catalyze CO_2RR. The role of this supporting layer (6 cm × 6 cm × 0.3 cm) is to hold the sapphire window (i.d. 12.7 mm). The entire assembly is sandwiched between the two stainless housings fastened with 8 bolts of 6.35 mm diameter.

Operando Raman Confocal Microscopy

Confocal Raman spectra were collected using a fiber-coupled Olympus BX-51 microscope with a 785 nm excitation source (Innovative Photonics Solutions I0785MM0350M64F). An average of 6

spectra per measurement with 5 seconds exposure times were acquired using a Princeton Instruments Acton SP2300 spectrograph and PIXIS-100 CCD camera with LightField software on Windows 7. A grating of 600 grooves/mm and resolution of 4.5 cm^{-1} dispersed the light onto the CCD camera, which was rotated over the course of acquisition to cover a window of interest from 400-2500 cm^{-1}. All spectra were processed in the same way using the house-written MATLAB code. A representative blank spectrum (acquired with the laser off) was subtracted from each spectrum to remove the CCD noise baseline and the constant contribution from hot-pixels. Next, the background was removed by fitting a 10^{th} order polynomial to the spectrum.[2] The minimum value between the spectrum and polynomial fit is kept, then fit again to a new polynomial. This process is repeated 40 times, producing a tight background approximation. Background corrected spectra are then filtered for high frequency noise using discrete wavelet transform. The first two levels of detail coefficients are removed using the symlet 5 wavelet. Each spectra is then normalized by the L2-norm.

Methods to Construct HCO_3^-/CO_3^{2-} ratios *via* Raman Spectra, and pH Calculations

For two Raman active species HCO_3^- and CO_3^{2-} in liquid phase, the relative concentrations are related to their Raman signal areas (*S*).[3–5] The signals at the wavenumbers of 1032 and 1080 cm^{-1} are assigned to HCO_3^- and CO_3^{2-} vibrational modes, respectively. Origin 2018 was used to integrate signal areas. The lowest intensity point (ν = 1070 cm^{-1}) between 1032 and 1080 cm^{-1} was chosen as the separation wavenumber between HCO_3^- signal and CO_3^{2-} signal. All spectra were processed in the same manner using the endpoint as the baseline for the integration, and a horizontal baseline for the signal integration. It is important to note that it is difficult to obtain the identical measuring condition (due to bubble generations), therefore, the ratio of signal integrations was used to calculate the pH at the surface of silver cathode. The $[HCO_3^-]$ / $[CO_3^{2-}]$ is related to their Raman signal areas (*S*), and the total carbon

concentration is conserved, therefore, the [HCO_3^-] and [CO_3^{2-}] can be determined. Finally, we used Davies equation to estimate pH values through the pH-dependent equilibrium of HCO_3^-/CO_3^{2-}. We experimentally validated the Davies equation in this system despite the high ionic strength. The pH values obtained from Raman spectra (after correction) are defined as the $pH_{surface}$. The pH in the bicarbonate solution reservoir was measured by a pH meter (Accumet AB150), which is defined as the pH_{bulk}.

[HCO_3^-] and [CO_3^{2-}] ratios are related to their Raman signal areas

We experimentally investigated the relationship between the Raman signals for HCO_3^- and CO_3^{2-} and their corresponding concentrations at high ionic strength solutions. Different ratios of $KHCO_3$ and K_2CO_3 were dissolved in deionized (DI) water (Table S1) and then tested with Raman spectroscopy. The signals at the wavenumbers of 1030 and 1080 cm^{-1} were assigned to HCO_3^- and CO_3^{2-} vibrational modes, respectively. Origin 2018 was used to integrate these signal areas, and the integration process is described in the Experimental section. The results show that the experimental initial ratios of [HCO_3^-] / [CO_3^{2-}] matched the Raman area ratios (Table S1).

Table S1. $KHCO_3$ and K_2CO_3 solutions prepared with different ratios and the corresponding Raman signal integral ratios.

$KHCO_3$ (mmol)	K_2CO_3 (mmol)	EDTA (g)	Volume (ml)	[HCO_3^-] / [CO_3^{2-}] (experimental)	Raman signal integral ratios
145.54	4.27	0.3	50	34	40.86
140.04	9.99	0.3	50	14	16.12
135.05	14.98	0.3	50	9	10.44

125.06	25.04	0.3	50	5	5.45
99.99	50	0.3	50	2	1.57

The pH calculations *via* the equilibrium of HCO_3^-/CO_3^{2-}

The pH values were calculated based on the equilibrium of HCO_3^-/CO_3^{2-}. It is important to note that it is difficult to obtain the identical measuring condition (due to bubble generations), therefore, the ratio of signal areas was used to calculate the pH on the focus spot. Single signals from different Raman spectra would not be directly used for any quantitative comparison. A calibration curve is not available in this situation either. The calculation was done with the *CurTiPot pH calculator* software.

The initial solution contains 3 M $KHCO_3$ and 0.02 M EDTA (H_4Y). pKa values of the corresponding conjugate acids (carbonic acid and EDTA (H_6Y^{2+})) are listed in **Table S2**. At the measured solution pH of ~8.5, EDTA is deprotonated to HY^{3-}, and the reaction occurs (**Eq. 1**):

$$HCO_3^- + H^+ = H_2O + CO_{2(g)} \qquad \textbf{Eq. 1}$$

Therefore, 2.94 M $KHCO_3$ and 0.02 M deprotonated EDTA (HY^{3-}) were used as the initial solution concentrations for the pH calculations. The estimate of pH is based on the inverse of the logarithm of the activity of H^+ ions (not concentrations) (**Eq. 2**):

$$pH = -\log aH^+ = -\log([H^+] \times \gamma H^+) \qquad \textbf{Eq. 2}$$

Where [H] and γH^+ represent the proton concentration (M) and proton activity coefficient respectively, which was estimated by the Davies equation (**Eq.3**) [6]:

$$\log \gamma = -A Z_i^2 \left(\frac{\sqrt{I_m}}{1+\sqrt{I_m}} - 0.2 I_m \right) \qquad \textbf{Eq. 3}$$

Where Z_i is the valence of ion i. Under standard conditions (water at 25°C), A can be calculated based on the **Eq. 4**

$$A=1.82\times10^{6}\times(\varepsilon T)^{-(3/2)} \quad \textbf{Eq. 4}$$

onic strength (I_m) is calculated from the concentrations of the ionic components (c_i) using **Eq. 5**

$$I_m = \tfrac{1}{2}\sum_i Z_i^2 c_i \quad \textbf{Eq. 5}$$

Therefore, the activity coefficient of species HCO_3^-, CO_3^{2-}, HY^{3-}, H_2Y^{2-}, H_3Y^- can be calculated respectively. Table S3 shows the activity coefficients calculated for ionic species at the concentration of $c_{HCO_3^-} = 2.94$ M, $c_{CO_3^{2-}} = 0$ M and $c_{HY^{3-}} = 0.02$ M. For each concentration of HCO_3^- and CO_3^{2-}, their corresponding activity coefficients have to be re-calculated (ɣ is concentration dependent). The concentrations of HCO_3^- and CO_3^{2-} can be calculated by the Raman signal integral (**Eqs. 6, 7**)

$$c_{HCO_3^-} = 2.94\times S_{HCO_3^-}/(S_{HCO_3^-} + S_{CO_3^{2-}}) \quad \textbf{Eq. 6}$$

$$c_{CO_3^{2-}} = 2.94\times S_{CO_3^{2-}}/(S_{HCO_3^-} + S_{CO_3^{2-}}) \quad \textbf{Eq. 7}$$

The pH values were then calculated using CurTiPot pH analysis and simulation software version 4.2 and the calculated $c_{HCO_3^-}$, $c_{CO_3^{2-}}$ and $c_{HY^{3-}}$. To validate the simulation results, different ratios of $KHCO_3$ and K_2CO_3 were dissolved in deionized (DI) water and their corresponding pH was measured by a pH meter, and was calculated through the above-mentioned method ($pH_{simulated}$) (**Table S4**). The results

showed the calculated pH is higher than the experimentally measured pH, and the $pH_{surface}$ values were modified by the experimentally measured difference by **Eq. 8**

$$pH_{surface}=pH_{simulated}-0.17 \quad \textbf{Eq. 8}$$

Although the Davies equation is considered to be suitable for the solutions with ionic strengths ≤0.5 M, it can predict the HCO_3^-/CO_3^{2-} system even in higher ionic strength with proper modifications (with an error of < 0.1 pH unit).

The pKa_1 and pKa_2 of carbonic acid are temperature dependent based on the **Eqs. 9** and **10**.[7]

$$pKa_1= 3404.71/T(K) + 0.032786T(K)-14.8435 \quad \textbf{Eq. 9}$$

$$pKa_2=2902.39/T(K) + 0.02379T(K)- 6.4980 \quad \textbf{Eq. 10}$$

At any temperature, the corresponding pKa_1 and pKa_2, and A (Eq 4) values were calculated and used $pH_{surface}$ calculations.. Finally, we used the Davies equation to calculate the $pH_{surface}$ values at different temperatures.

Table S2. pKa values of the carbonic acid and EDTA in aqueous solutions.

Acid	**H_2CO_3**	**EDTA (H_6Y^{2+})**
pKa_1	6.35	-0.210
pKa_2	10.33	1.500
pKa_3	NA	2.210
pKa_4	NA	3.110

pKa_5	NA	6.750
pKa_6	NA	11.030

Table S3. The activity coefficient of species at the concentration of $c_{HCO_3^-}$=2.94 M, $c_{CO_3^{2-}} = 0$ M and $c_{HY^{3-}} = 0.02$ M in aqueous solutions based on the Davies equation.

Activity coefficient	**Carbonic acid**	**EDTA (H_6Y^{2+})**
ɣY (Y: conjugate acid base)	0.889	0.624
ɣHY	0.971	0.767
$ɣH_2Y$	1.000	0.889
$ɣH_3Y$	NA	0.971
$ɣH_4Y$	NA	1.000

Table S4. The measured pH and simulated pH values for different ratios of $KHCO_3$ and K_2CO_3 solutions. The c_{total} is 3 M with 0.02 M EDTA.

$c(HCO_3^-)/c(CO_3^{2-})$ (experimental)	**Measured pH**	**pH_{Raman} (before modification)**	**$pH_{surface}$ (after modification)**
83	8.57	8.69	8.52
29	8.84	8.98	8.81
14	9.17	9.28	9.11
9	9.30	9.49	9.32
5	9.70	9.84	9.67

2	10.04	10.30	10.13
1	10.46	10.68	10.51

Table S5. pKa1 and pKa2 values at different temperatures

Temperature (℃)	pKa1	pKa2
20	6.38	10.38
37	6.30	10.22
56	6.30	10.14
70	6.37	10.12

The amount of escaped CO_2 calculation

For all experiments carried out in this study, a 125 ml 3M $KHCO_3$ was used as the cathodic feedstock. A 15 min electrolysis at 50 mA cm^{-2} was monitored by operando Raman. During the process, the amount of produced CO_2 (Eq 11) was calculated by the following equation:

$$n_{CO2}=j \times S \times t/F \qquad \textbf{Eq. 11}$$

J is current density (50 mA cm^{-2}) and S represents the electrode physical surface area (4 cm^2). F is Faraday constant (96485.33 C mol^{-1}). Therefore, the produced CO_2 is 0.00186 mol, occupying 0.49% of the total carbon amount for the overall feedstock.

Figure S1. Optical images of the bicarbonate flow cell for operando Raman measurements

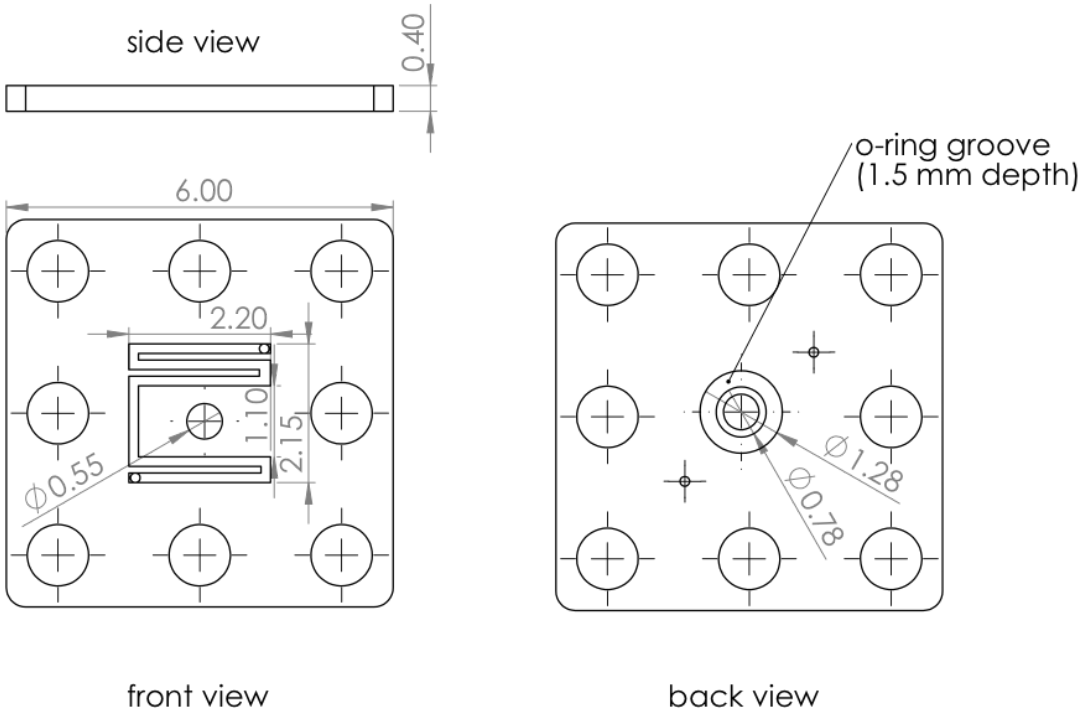

Figure S2. Dimensions of the cathode flow plates. All dimensions are in cm.

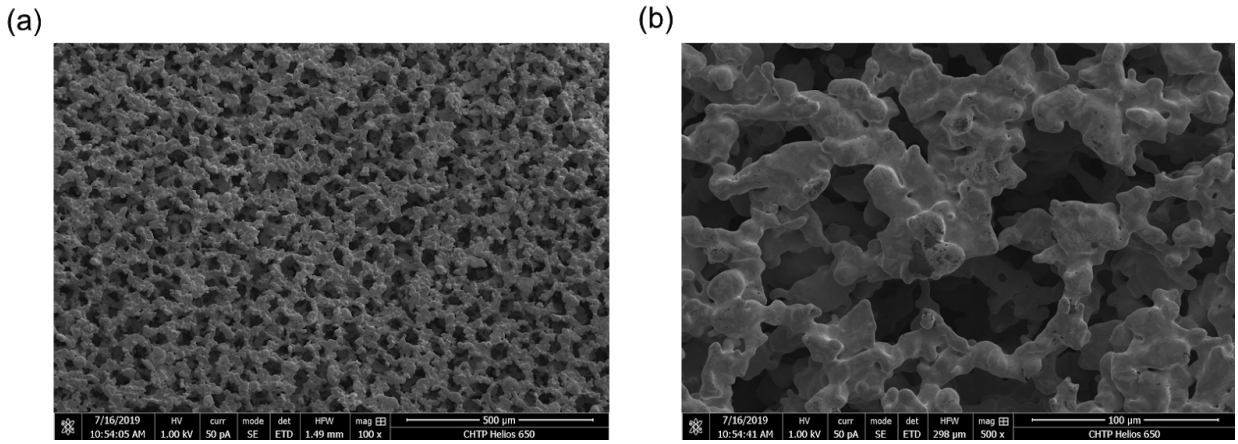

Figure S3. SEM images of the free-standing silver foam electrode with different magnifications.

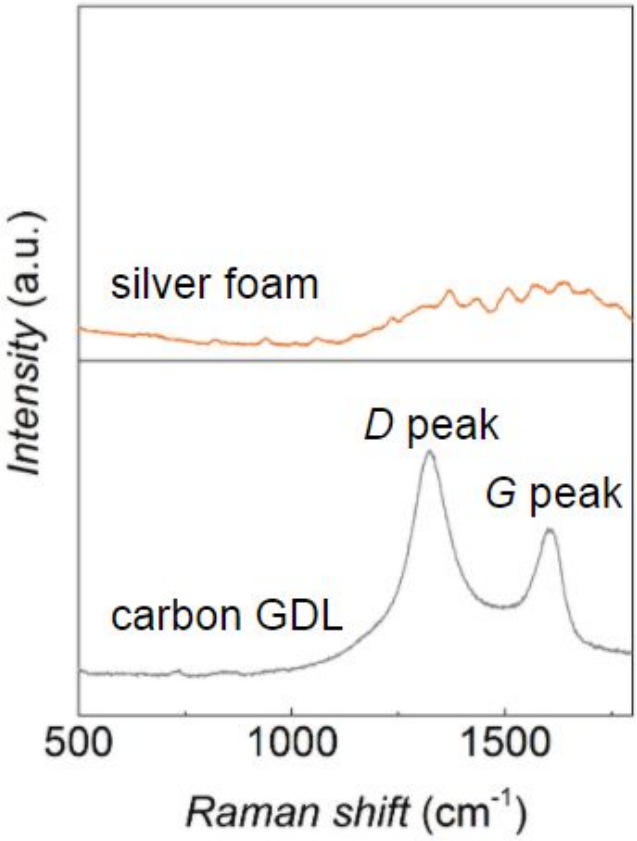

Figure S4. Raman spectra of silver foam and carbon gas diffusion layer (GDL, Cetech®) at the focal spot. The Raman spectrum of carbon GDL shows the D and G peaks at 1320 and 1620 cm^{-1}.

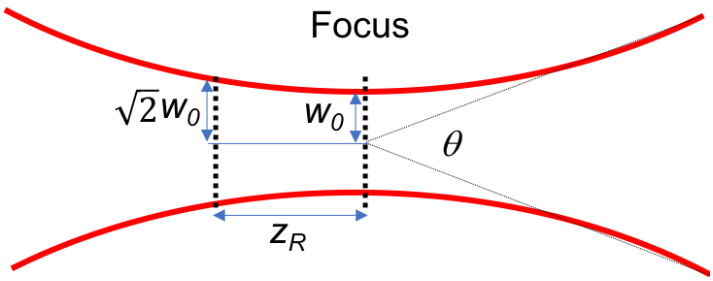

Figure S5. The calculated spot size and focal depth of the Raman beam based on Gaussian beam laws, where Z_R is the distance from the beam waist to where the beam area doubles compared with the waist area, and W_0 is the radius of the beam waist size. $W_0 = \frac{\lambda n^{-1}}{\pi NA}$; $Z_R = \frac{\pi W_0^2}{\lambda n^{-1}}$; λ is the Raman wavelength (785 nm) and n is the index of refraction of water (1.33); The calculated spot size is 2.04 and the focal depth is 11 μm.

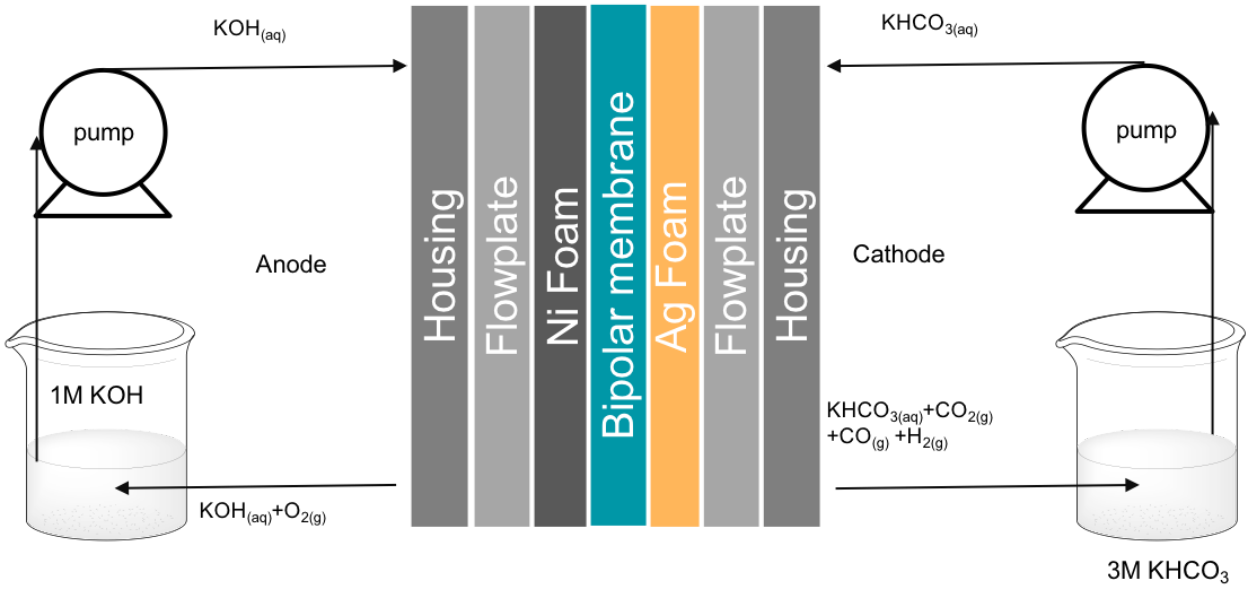

Figure S6. Experimental setup of the flow cell experiment.

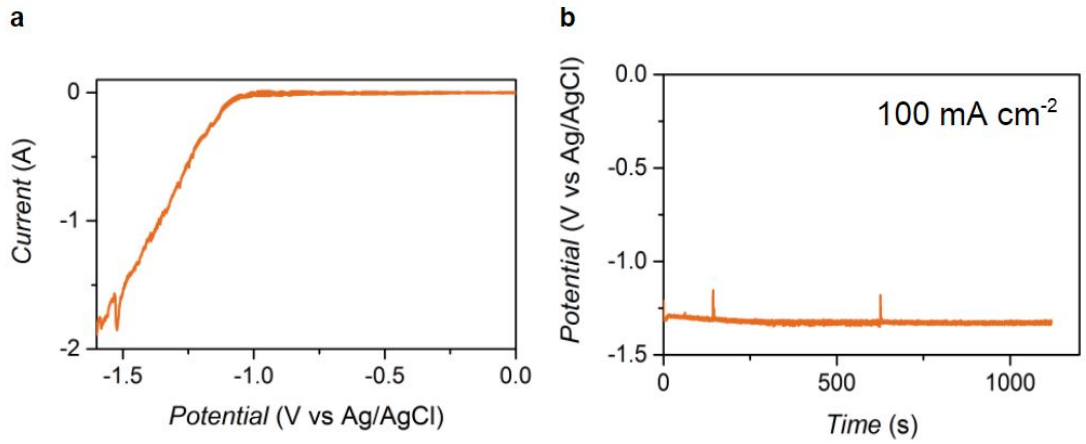

Figure S7. (a) Linear sweep voltammetry (LSV) curve acquired in the modified flow cell with 3 M $KHCO_3$ feedstock. The cathode potential was measured by inserting a reference electrode in the inlet of the catholyte tube. (b) Cathode potential- time curve acquired in the modified flow cell with 3 M $KHCO_3$ feedstock at 100 mA cm^{-2}.

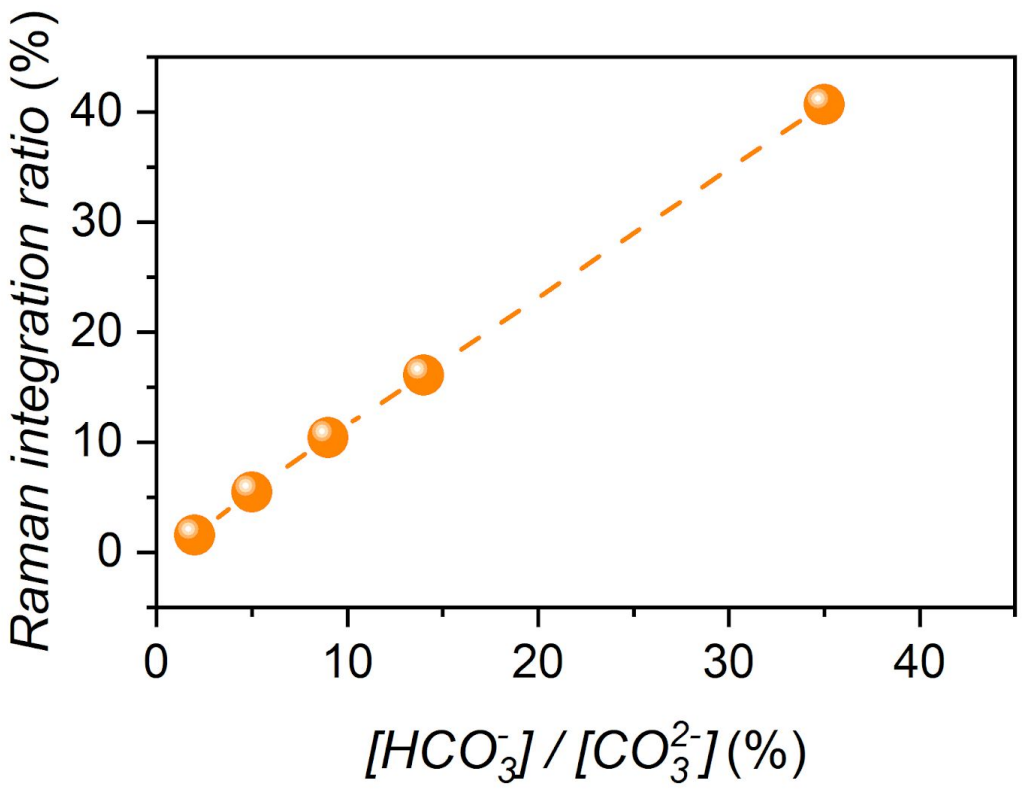

Figure S8. Independent control experiments on bulk solutions confirmed that the relative concentrations of $[HCO_3^-]$ to $[CO_3^{2-}]$ corresponds to the ratio of the HCO_3^- signal ($S_{bicarbonate}$) to the carbonate signal ($S_{carbonate}$) measured by Raman spectroscopy

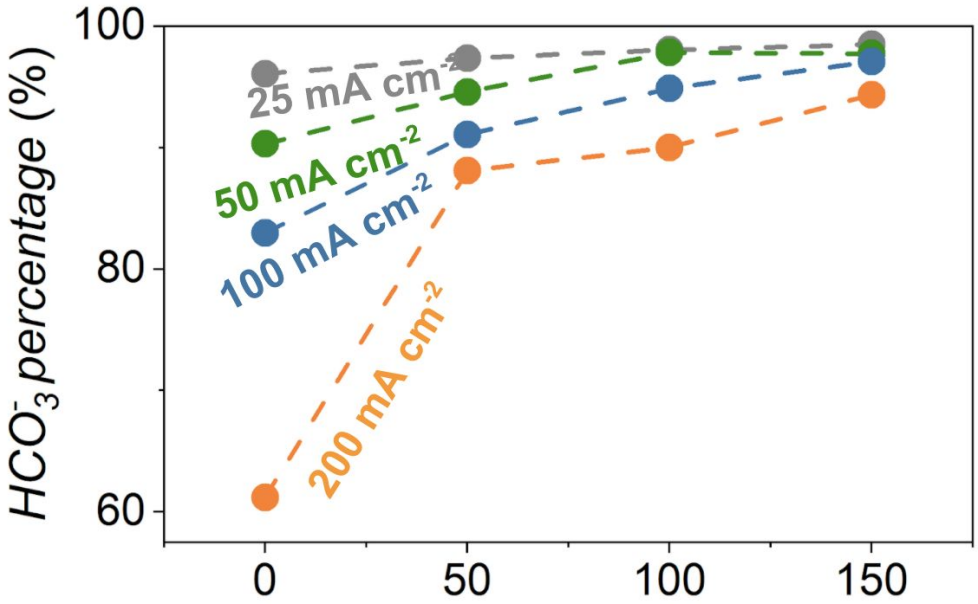

Figure S9. Constructed HCO_3^- concentrations at different distances from the Ag surface at different current densities (25, 50, 100 and 200 mA cm^{-2}). All data were collected at t = 300 s.

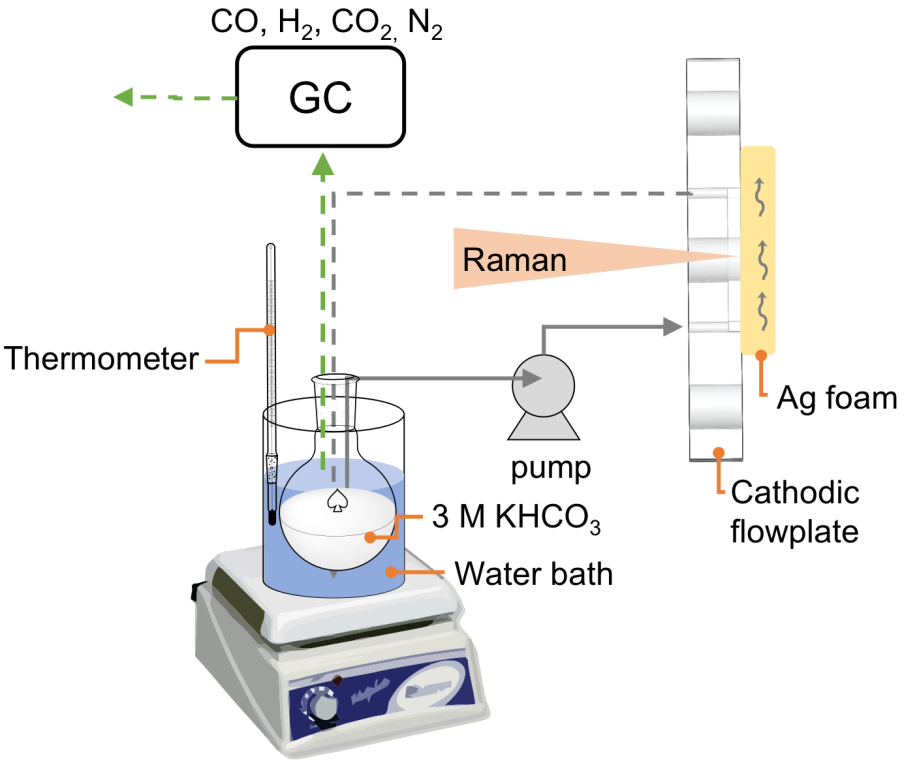

Figure S10. Illustration of the experimental setup that the bicarbonate reservoir is heated and the feedstock and inlet temperature are measured by a glass thermometer and a resistant thermal detector (RTD) respectively. An in-line GC is coupled to analyze the gaseous products.

References

(1) Li, T.; Lees, E. W.; Goldman, M.; Salvatore, D. A.; Weekes, D. M.; Berlinguette, C. P. Electrolytic Conversion of Bicarbonate into CO in a Flow Cell. *Joule* **2019**, *3* (6), 1487–1497.
(2) Galloway, C. M.; Le Ru, E. C.; Etchegoin, P. G. An Iterative Algorithm for Background Removal in Spectroscopy by Wavelet Transforms. *Appl. Spectrosc.* **2009**, *63* (12), 1370–1376.
(3) Wu, J.; Zheng, H. Quantitative Measurement of the Concentration of Sodium Carbonate in the System of Na2CO3–H2O by Raman Spectroscopy. *Chem. Geol.* **2010**, *273* (3), 267–271.
(4) Wopenka, B.; Pasteris, J. D. Limitations to Quantitative Analysis of Fluid Inclusions in Geological Samples by Laser Raman Microprobe Spectroscopy. *Appl. Spectrosc., AS* **1986**, *40* (2), 144–151.

(5) Frantz, J. D. Raman Spectra of Potassium Carbonate and Bicarbonate Aqueous Fluids at Elevated Temperatures and Pressures: Comparison with Theoretical Simulations. *Chem. Geol.* **1998**, *152* (3), 211–225.
(6) Sun, M. S.; Harriss, D. K.; Magnuson, V. R. Activity Corrections for Ionic Equilibria in Aqueous Solutions. *Can. J. Chem.* **1980**, *58* (12), 1253–1257.
(7) Harned, H. S.; Davis, R. The Ionization Constant of Carbonic Acid in Water and the Solubility of Carbon Dioxide in Water and Aqueous Salt Solutions from 0 to 50°. *Journal of the American Chemical Society* **1943**, *65* (10), 2030–2037.